Available online at www.sciencedirect.com

ScienceDirect

Genomics 91 (2008) 443–450

GENOMICS

www.elsevier.com/locate/ygeno

Hypomethylated and hypermethylated profiles of *H19*DMR are associated with the aberrant imprinting of *IGF2* and *H19* in human hepatocellular carcinoma

Jing Wu [a,b,1], Yang Qin [a,b,*], Bo Li [c,*], Wen-zhi He [a], Zhi-lin Sun [a]

[a] *Department of Biochemistry and Molecular Biology, School of Preclinical and Forensic Medicine, West China Medical Center, Chengdu 610041, Sichuan Province, China*

[b] *State Key Laboratory of Biotherapy, Sichuan University, Chengdu 610041, Sichuan Province, China*

[c] *Department of General Surgery, West China Medical Center, Chengdu 610041, Sichuan Province, China*

Received 8 October 2007; accepted 18 January 2008

Available online 20 March 2008

Abstract

In this study, 39 human hepatocellular carcinoma (HCC) tissues and 7 normal adult liver tissues were screened for heterozygous polymorphisms in *IGF2, H19,* and the differentially methylated region of *H19* (*H19*DMR) using PCR–RFLP and PCR sequencing. The imprinting of *IGF2* and *H19* was examined by RT-PCR–RFLP, while the methylation profile of *H19*DMR was detected by bisulfite sequencing from every informative sample. Of the informative HCC samples 47.06% (8 of 17) demonstrated a gain of imprinting of *IGF2,* and 21.74% (5 of 23) of the informative HCC samples demonstrated a loss of imprinting of *H19.* Interestingly, we found three methylation profiles for *H19*DMR in the informative HCC samples: hyper-, medium-, and hypomethylated profiles. Furthermore, the hypomethylated and hypermethylated profiles were immediately associated with aberrant imprinting of *IGF2* and *H19.*

Keywords: Methylation; Imprinting; *IGF2*; *H19*; Human hepatocellular carcinoma; Liver

Genomic imprinting is the preferential silencing of one parental allele due to epigenetic modifications. Insulin-like growth factor 2 (*IGF2*) and *H19* are two imprinted genes located adjacent to each other at chromosome 11p15.5 in humans. *IGF2,* which encodes a protein functioning as a fetal growth factor and a cell mitogen, is expressed only from the paternal allele in most tissues [1,2]. *H19,* which acts as an RNA, is a gene of unknown function and expressed only from the maternal allele [3,4].

The mechanism of imprinting of *IGF2* and *H19* is not clearly revealed. One understanding is that differentially methylated regions (DMRs) may act as epigenetic modifiers of allelic expression by recruiting proteins specifically binding to methylated or unmethylated DNA [5–10], which come after an experimental deletion in mice of a region upstream of *H19.* This most notable region is *H19*DMR, which is methylated only on the paternal allele in both mouse and human [5] and is regarded as a key domain for the control of imprinting of *IGF2* and *H19* because deletion of this region results in loss of imprinting of both *IGF2* and *H19* [6]. This region contains four specific binding sites for a vertebrate enhancer-blocking protein CTCF (CCCTC-binding factor) in the mouse, while it contains seven CTCF binding sites in human [7–9]. One of the putative explanations for imprinting is the enhancer competition model, in which *IGF2* and *H19* promoters compete with each other on the same chromosome for a set of shared *H19* downstream enhancers, while CTCF binds the unmethylated maternal allele and acts as an insulator between the *IGF2* promoter and the enhancers, thereby suppressing *IGF2* transcription maternally. Methylation of the paternal allele prevents CTCF binding, thereby precluding the establishment of the insulator and allowing *IGF2* transcription paternally [10].

Abnormal imprinting of *IGF2* and/or *H19,* resulting in a gain or loss of imprinting, commonly occurs in various types of cancer and may be involved in malignant transformation [11]. Gain of imprinting (GOI) is the setting up of the "mark" causing

* Corresponding authors. Y. Qin is to be contacted at fax: +86 28 85501243. B. Li, fax: +86 28 85423724.

E-mail addresses: qin_1@sina.com (Y. Qin), cdlibo@medimail.com.cn (B. Li).

[1] Current address: The Sixth People's Hospital, HangZhou, China.

0888-7543/$ - see front matter © 2008 Elsevier Inc. All rights reserved.
doi:10.1016/j.ygeno.2008.01.007

expression of either the maternal or the paternal allele, whereas loss of imprinting (LOI) is the removal of the "mark," leading to biallelic expression of genes. The mechanisms for GOI and LOI are not elucidated, although a large number of studies have been focused on the modification of DMRs [12–16]. In Wilms' tumor, it was shown that the aberrant hypermethylation of a CTCF binding site within *H19*DMR was necessary but not sufficient for LOI of *IGF2* [12]. And in colorectal cancer, one study reported that LOI of *IGF2* correlated strongly with maternal hypermethylation of the sixth CTCF binding site in *H19*DMR [13]. However, another report suggested that hypomethylation of the paternal DMR within *IGF2* intron 2 but not the *H19*DMR was a mechanism for *IGF2* LOI in human colon [14]. Additionally, hypomethylation in the paternal *H19*DMR was found in partial bladder cancer tissues even without *H19* LOI and without the message of the imprinting of *IGF2* [15]. More interestingly, in osteosarcoma, it was demonstrated that *IGF2* LOI occurred with biallelic CpG hypermethylation of *H19*DMR, while *H19* LOI was accompanied by biallelic hypomethylation of this region, and the methylation status of *IGF2*DMR was not uniform [16].

In human liver, the mechanism of imprinting of *IGF2* and *H19* would be more complicated because *IGF2* is paternally expressed in fetal liver but changes to biallelic expression in adult liver. This would result from the promoter usage [17,18]. The human *IGF2* gene contains four tissue- and developmental-specific regulation promoters (P1–P4) [17]. The P1 promoter is silenced in fetal liver but activated after birth and gradually up-regulated to produce approximately 50% of the total *IGF2* mRNA in normal adult liver, while in the majority of other tissues it remains silenced even in the adult. The P3 promoter is the most active promoter in fetal and newborn human liver and produces approximately 70% of the total *IGF2* transcripts in this developmental stage of the liver, while it is silenced in the majority of normal adult livers. Normally, P1 activity is always biallelic, whereas the other three promoters drive transcription from only one allele [18].

It has been demonstrated that dysregulated expression of *IGF2* and/or *H19* is involved in the hepatocarcinogenesis [19–21], and both DNMT1 and DNMT3a are strikingly up-regulated in human hepatocellular carcinoma (HCCs) [22,23]. Although the aberrant imprinting of *IGF2* was first observed many yeas ago [24], there are few reports focused upon the mechanism of imprinting regulation in HCCs. In this study we used bisulfite sequencing to investigate the methylation status of *H19*DMR in HCC tissues compared with normal adult liver tissues and study the relationship between the methylation profile and the allelic expression of *IGF2* and *H19*.

Results

Genotypes of IGF2, H19, and H19DMR in HCC

The schematics of *IGF2, H19,* and *H19*DMR polymorphisms detected in this study are shown in Fig. 1. By PCR and RFLP analysis, all 7 normal liver and 17 of 39 HCC samples were heterozygous for ApaI polymorphism in *IGF2* exon 9, while all 7 normal liver and 23 of 39 HCC samples were

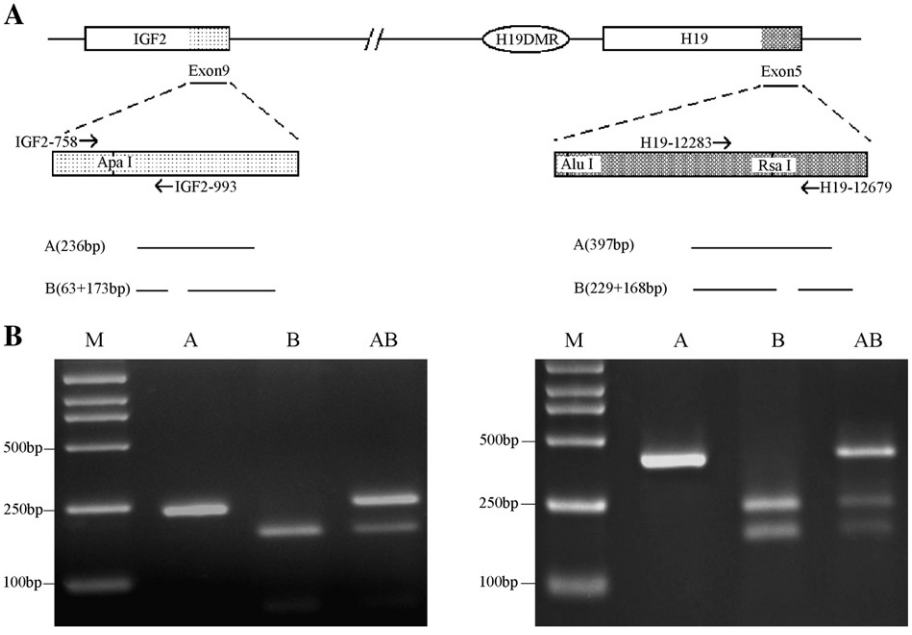

Fig. 1. *IGF2* and *H19* polymorphisms. (A) Schematic of the *IGF2*/*H19* region of chromosome 11p15.5. Locations of PCR primers are indicated by arrows. The polymorphism was analyzed in *IGF2* exon 9 (ApaI at bp 819); *IGF2* bases are numbered as found in GenBank Accession No. X07868 (gi: 32998). The polymorphism was analyzed in *H19* exon 5 (RsaI at bp 12511); *H19* bases are numbered as found in GenBank Accession No. AF125183 (gi: 4731323). IGF2-758, IGF2-993, H19-12283, and H19-12679 represent PCR primers for amplification of *IGF2* and *H19*. Predicted products for the A and B alleles of each polymorphism are drawn below the schematic. (B) Actual products of genotype analysis. Representative samples of A homozygotes, B homozygotes, and AB heterozygotes are shown for each polymorphism, according to the above schematic.

informative for *H19* at RsaI and/or AluI in exon 5 (Fig. 1B). The genotypes of *H19*DMR at three SNPs were determined by PCR sequencing for 39 HCC and 7 normal liver tissues. Overall 20 HCCs and 5 normal liver samples were heterozygous in at least one of the three polymorphisms of *H19*DMR.

Allelic expression of IGF2 and H19 in HCC

To determine the imprinting status, we analyzed the informative samples for *IGF2* and *H19* allelic expression by RT-PCR and RFLP. The results of allelic expression in HCC and normal liver samples are listed in Table 1 and the typical samples are shown in Fig. 2. All 7 normal liver samples informative for *IGF2* showed biallelic expression of *IGF2,* while 8 of 17 HCC informative samples showed abnormal monoallelic expression of *IGF2,* which was so-called gain of imprinting of *IGF2,* and the remaining 9 HCC samples showed seemingly normal biallelic expression of *IGF2.* Regarding the *H19* gene, all 7 informative normal liver samples showed generally accepted normal monoallelic expression, while 5 of 23 informative HCC samples showed abnormal biallelic expression of *H19,* which was so-called loss of imprinting, and the other 17 HCCs showed seemingly normal *H19* imprinting. Among all of the HCC tissue samples, 12 (12/26; 46.2%) showed the aberrant imprinting for at least one of the *IGF2* and *H19* genes, suggesting that the aberrant imprinting expression of *IGF2* and *H19* is a common phenomenon during hepatocellular carcinogenesis.

To address whether the abnormal imprinting of *IGF2* was correlated with aberrant imprinting of *H19,* we analyzed the relationship between the imprinting of *IGF2* and *H19.* In the 14 HCC cases informative for both *IGF2* and *H19,* variable patterns of reciprocal imprinting expression were exhibited: 5 cases with *IGF2* GOI and normal monoallelic expression of *H19,* 2 cases with seemingly normal biallelic expression of *IGF2* and *H19* LOI, 6 cases with seemingly normal biallelic *IGF2* expression and normal monoallelic *H19* expression, and 1 case with *IGF2* GOI and *H19* LOI. No significant correlation was observed between the allelic expression of *IGF2* and *H19* ($p > 0.05$).

Table 1
Summary of the imprinting alterations of *IGF2/H19* and the average methylation of *H19*DMR in normal liver and HCC tissues

Sample	*IGF2* GOI	*H19* LOI	Average methylation (%)
NL1	No	No	51.33
NL2	No	No	Homo
NL4	No	No	Homo
NL5	No	No	48.00
NL6	No	No	41.60
NL7	No	No	44.00
NL8	No	No	51.50
HCC216	No	Yes	77.20
HCC212	No	No	72.80
HCC303	Yes	No	71.56
HCC213	Homo	Yes	70.00
HCC209	Yes	Homo	61.82
HCC126	Homo	Yes	60.40
HCC214	Yes	No	58.18
HCC115	Yes	No	55.60
HCC304	Yes	Homo	53.67
HCC220	No	No	50.80
HCC111	No	No	48.44
HCC206	Homo	No	46.55
HCC218	Homo	No	45.60
HCC128	No	No	44.40
HCC217	Homo	No	43.60
HCC117	No	No	39.60
HCC119	Yes	Yes	37.60
HCC116	Homo	No	36.50
HCC124	Yes	No	35.60
HCC129	No	Yes	1.14
HCC208	No	No	Homo
HCC114	Yes	No	Homo
HCC123	Homo	No	Homo
HCC125	Homo	No	Homo
HCC202	Homo	No	Homo
HCC301	No	Homo	Homo

Samples are listed with their unique numbers. Thirteen samples were uninformative and were not listed to conserve space. Average methylation, percentage of methylated CpG's in all analyzed CpG's; NL, normal liver sample; HCC, HCC sample; Homo, homozygous sample of the corresponding SNP site.

Methylation profile of H19DMR in HCC

We analyzed the methylation status of the potential *H19*DMR containing the sixth CTCF-binding site (CBS6) in HCC tissues and normal adult liver tissues by bisulfite sequencing. Three SNPs, but not CpG's, in this region allowed categorization of clones into groups based on allele of origin. The target fragment included 27 CpG's, of which the 8th and the 26th CpG's were excluded when we calculated the methylation rate because these two CpG's were potential C/T polymorphisms as well (Fig. 3).

A broken-line graph was drawn to show the methylation profiles of the normal liver and HCC samples clearly. The methylation rate of each CpG site was calculated and presented by a point, and two adjacent points were linked by a line (Fig. 4). The sum of all 25 CpG sites' methylation rate divided by 25 was the average methylation of every sample. In all informative normal liver cases, a medium-methylated profile was observed in the target region (Fig. 4A). The average methylation ranged from 41.60 to 51.50% (47.28±8.63%, $n=5$) (Table 1); in other words, one allele was nearly all methylated, whereas the other was almost unmethylated (Fig. 3B). The high variability in methylation levels in consecutive CpG's among individuals led to surprisingly complex methylation patterns in 20 informative HCC cases. The average methylation in HCCs ranged from 1.14 to 77.20%, even though the majority of them maintained the allelic differential methylation(Table 1). The methylation profiles could be grouped into three discrete methylation categories in HCC samples compared with normal liver samples: a hypermethylated profile (average methylation > 51.50%: 64.59±16.54%, $n=9$), a medium-methylated profile (41.60% < average methylation < 51.50%: 46.80±5.17%, $n=6$), and a hypomethylated profile (average methylation < 41.60%: 30.00±31.77%, $n=5$). The sequencing results from three typical HCC samples corresponding to each of the three different methylation profiles are shown in Figs. 3B and 4B.

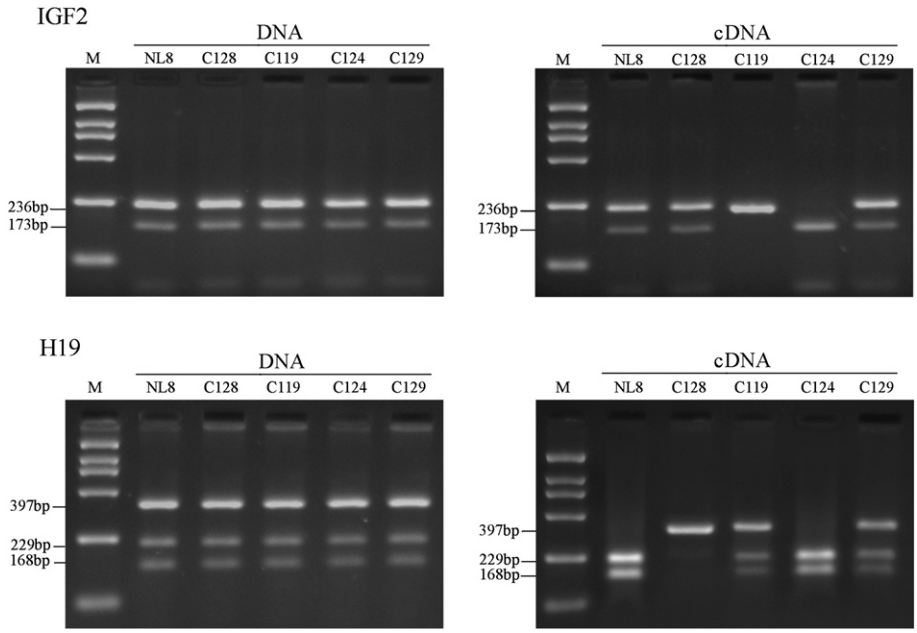

Fig. 2. Genotyping and allelic expression of *IGF2* and *H19* of representative samples. Representative samples of normal liver (sample NL8), normal imprinting of *IGF2* and *H19* (sample HCC128), *IGF2* GOI with *H19* LOI (sample HCC119), *IGF2* GOI with normal *H19* imprinting (sample HCC124), and *H19* LOI with normal *IGF2* imprinting (sample HCC129) are presented. The "DNA" gels show the results of genotyping for the *IGF2* and *H19* polymorphisms studied. The "cDNA" gels show the results of allelic expression analysis by RT-PCR–RFLP.

Relationship between H19DMR methylation profile and imprinting of both IGF2 and H19 in HCC

To address the question whether the three methylation profiles at the sixth CTCF binding site had an effect on the allele-specific expression of either *IGF2* or *H19* in HCC, we analyzed the relation between *IGF2* GOI or *H19* LOI and methylation profile. No obvious correlation was observed for either of them ($p > 0.05$). However, we found an interested tendency when both *IGF2* GOI and *H19* LOI were integrated into one group: all the abnormal imprinting samples were distributed to either the hypermethylated group or the hypomethylated group. When the HCCs were arranged in average methylation order, it could be easily seen that the samples with abnormal imprinting of *IGF2* and/or *H19* were located at the two ends (Table 1). This tendency was more distinct for the first 21 CpG's (Fig. 4). It was demonstrated that both hypermethylation and hypomethylation were associated with abnormal imprinting of *IGF2* and/or *H19* ($p < 0.003$).

Discussion

Aberrant imprinting status of *IGF2* and/or *H19* commonly occurs in human cancers, while the dysregulation mechanism remains elusive. In the mouse, the *H19*DMR is required for both *IGF2* and *H19* imprinting [6]. The classical competition model suggests that the unmethylated maternal *H19*DMR allows CTCF binding, establishing an insulator to prevent *IGF2* transcription and support *H19* transcription. In contrast, the methylated paternal *H19*DMR allows for *IGF2* transcription and prevents *H19* transcription [8,9]. However, this model cannot explain many alterations of imprinting occurring in human cancers [12–16].

In this study, we examined the imprinting status of *IGF2* and *H19;* 47.1% of HCC cases demonstrated GOI of *IGF2* and 26.1% of HCC cases showed LOI of *H19. IGF2* GOI and *H19* LOI occurred at more significant frequencies in HCCs than in the normal liver samples, which is consistent with previous reports [24,27], indicating that *IGF2* GOI and *H19* LOI could be markers for detection of HCC. As we mentioned previously, *IGF2* has four promoters and normal P1 activity is always biallelic, whereas other three promoters' activity drives transcription from only one allele. Biallelic expression of *IGF2* could not be judged as "normal" because the abnormal biallelic activation of the P2, P3, or P4 could cause a similar result. And abnormally silenced P1 promoter as well as a reactivated P3 promoter was found in HCC previously [24]. Moreover, our results show no striking interrelation of the two genes, supporting the idea that the *H19* transcript itself has no effect on the imprinting of its neighboring genes, which is derived from research in mice, despite the fact that noncoding RNA has been demonstrated to be involved in parent allelic expression at some loci in mammals [28].

Previously, one group found genome-wide hypomethylation in HCCs [22]; another Italian group demonstrated that the loss of maternal-specific methylation at the *Kv*DMR1 locus was common to a variety of adult neoplasms, including liver, breast, cervical, and gastric carcinomas [29]; and it has been reported that loss of parental-specific methylation at the *IGF2* exon 8–9 locus was specifically associated with HCC [30]. Conversely, one report demonstrated maternal hypermethylation upstream of *H19* in hepatoblastoma [31]. In this study we first used bisulfite sequencing to investigate the methylation status of *H19*DMR in HCC compared with normal liver control and analyzed the result combined with the allelic expression of *IGF2* and *H19.* Our findings

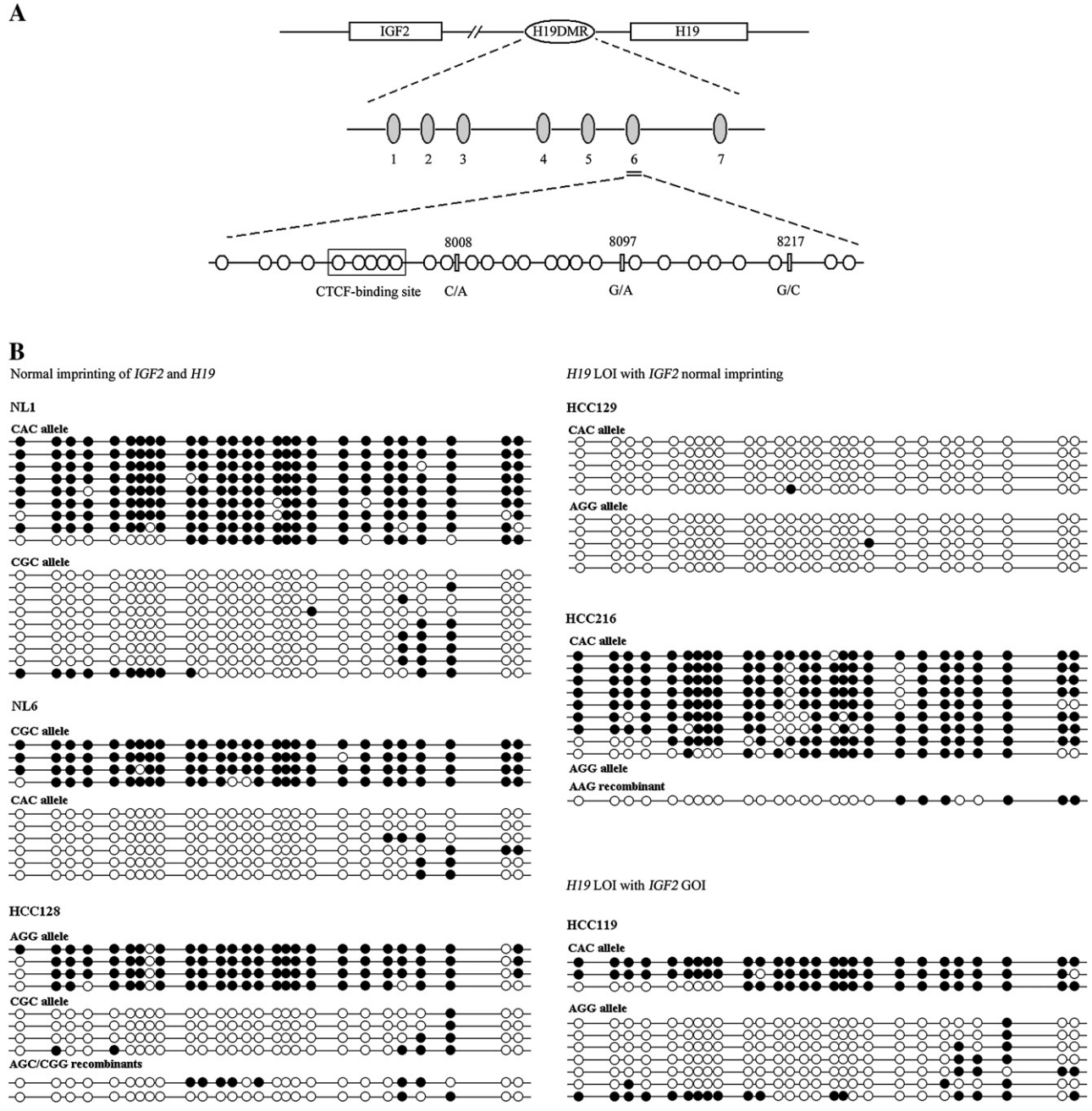

Fig. 3. Methylation status of individual CpG dinucleotides as determined by bisulfite sequencing. (A) Sketch map of the human *H19*DMR. An enlarged diagram is given for each cloned segment. Circles represent the locations of CpG dinucleotides. The locations of single-nucleotide polymorphisms, allowing for the identification of alleles, are represented by rectangles. Base numbering was performed according to GenBank Accession No. AF125183 (gi: 4731323). In our studied region, there are 25–27 CpG sites (CpG sites 8 and 26 are polymorphic; C/T). CpG sites 5–9 are located in the core region of the sixth CTCF-binding site. (B) Allele-specific methylation status of each CpG in every individual. Each line represents one cloned segment, black circles represent methylated CpG's, and white circles represent nonmethylated CpG's. In every individual, one genotype with methylated CpG sites represents an allele, another genotype represents another allele, and "recombinant" represents the mosaic genotype.

suggested that the abrupt medium-methylated profile at the sixth CTCF-binding site within *H19*DMR was immediately associated with the abnormal imprinting of *IGF2* and *H19*.

Although some reports suggested that the maternal hypermethylation at the six binding sites of CTCF within *H19*DMR may result in the loss of imprinting of *IGF2* in several types of cancers [12,13,16], no significant correlation was observed between the *IGF2* GOI and the hypermethylation or hypomethylation at the same region in our results. Both biallelic and monoallelic expression of *IGF2* was demonstrated whatever the methylation status of *H19*DMR in these examined HCC tissues. We could not neglect the influence of the different promoters' usage and other epigenetic modification before engaging in further experiments, because the promoters, the DMR in *IGF2,* and histone modification play a role in gene imprinting [14,32].

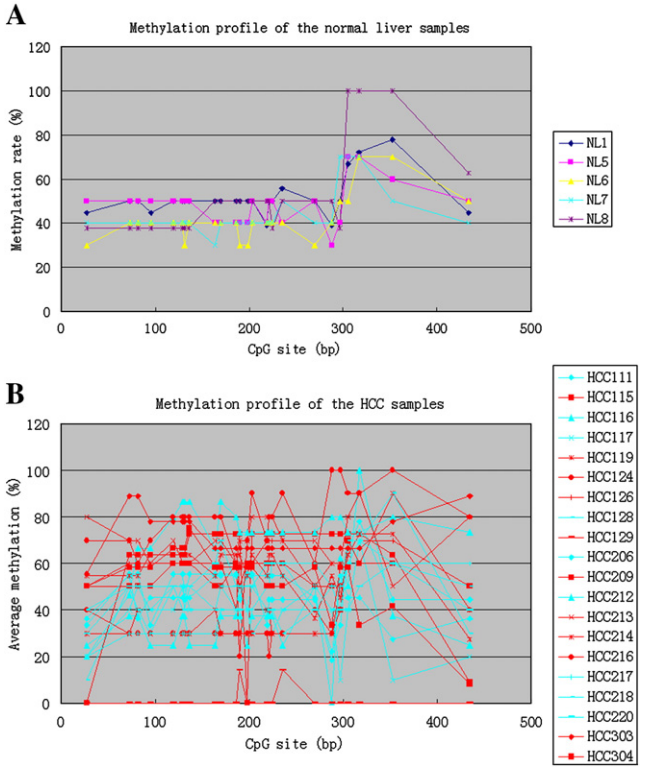

Fig. 4. Methylation profiles of *H19*DMR obtained by bisulfite sequencing. (A) Normal liver samples ($n=5$). (B) HCC samples ($n=20$). HCC samples with IGF2 GOI and/or H19 LOI are highlighted by a red broken line, and others are shown by a blue broken line.

The methylated paternal *H19*DMR contains a silencer element responsible for repression of *H19* [33], which could recruit a histone deacetylase through MeCP2 and Sin3a to repress the chromatin [34]. Nora Engel et al. introduced nine point mutations into *H19*DMR to deplete the CpG repeats of the CTCF-binding sites, and they demonstrated that paternal inheritance of the mutations resulted in biallelic expression of *H19*. This confirmed that the methylation of paternal *H19*DMR is necessary for *H19* imprinting [35]. Our study showed that demethylation of paternal *H19*DMR was linked with LOI of *H19,* but there were still several individuals with *H19* LOI displaying allelic differential methylation of the *H19*DMR locus. This is consistent with the idea that CTCF binding at the *IGF2/H19* imprinting control region is insufficient to regulate the expression of the two genes in many human tissues, and even CTCF may be not the only one of several factors involved in the regulation of genomic imprinting in human cancer [12,36]. We need further research on more cases to reveal the mechanism of imprinting.

Moreover, we found that the majority of samples, even including normal liver, displayed one or more clones with a "mosaic" pattern of methylation. The proved reason for this was that maternal/paternal heteroduplex products were created during the PCR step of the assay, and after being transmitted into *Escherichia coli* during the clone procedure, they would be randomly repaired by the bacterial mismatch repair system [37]. Using sequencing, some mosaic clones proved to be recombinants as a consequence of the in vivo repair process of heteroduplexes (Fig. 3B).

The major result in this study was that three degrees of methylation were first identified in HCCs and the medium-methylated samples accompanied seemingly normal imprinting, while the hyper- and hypomethylated samples usually accompanied *IGF2* GOI and/or *H19* LOI. To judge whether the hyper- and hypomethylated profiles in HCC are abnormal requires more cases. Nevertheless, it was confirmed that the hyper- and hypomethylated profiles were strongly associated with the abnormal imprinting of *IGF2* and *H19*. Many factors might be involved in the mechanism of imprinting regulation in vivo, so we could not explain the abnormal imprinting of *IGF2* and *H19* in HCC using any putative model alone. The revelation of the imprinting mechanism requires even more effort.

Materials and methods

Sample collection and nucleic acid isolation

With informed consent of patients, surgically resected tissues from 39 HCCs from unrelated patients and normal liver tissues from 7 unrelated accidental deaths were collected in The West China Hospital, Sichuan University, China. All specimens were confirmed histopathologically. Samples were flash frozen and stored at −80 °C until used in molecular biology studies. Genomic DNA was extracted using standard procedures by treatment with proteinase K and phenol–chloroform extraction, and total RNA was extracted using the single-step guanidium thiocyanate/acid phenol–chloroform standard method [25].

Genotyping of IGF2, H19, and H19DMR polymorphisms

One potential *IGF2* polymorphism, two potential *H19* polymorphisms, and three potential *H19*DMR polymorphisms are diagrammed in Figs. 1A and 3A. Genomic DNAs of all 46 samples were analyzed for the above six SNPs by PCR and RFLP to identify heterozygous samples of *IGF2, H19,* and *H19*DMR, respectively or sequencing. The PCR primer pairs, their optimal annealing temperatures, and the sizes of the PCR products were listed in Table 2. Each PCR was performed on a Mygene25 plus thermal cycler (LongGene, China) in a 25-μl volume containing 2.5 μl of PCR buffer (Sangong, China), 250 μM dNTPs, 20 pM appropriate primers, 1 U of Taq DNA polymerase (Sangong), and 300 μg of genomic DNA. PCR conditions were denaturing at 95 °C for 5 min, followed by 30 cycles of 95 °C for 30 s, optimal annealing temperature for 40 s, and 72 °C for 30 s, and finally 72 °C for 10 min. Then, the PCR products were digested by the corresponding restriction enzyme (ApaI, RsaI, or AluI) and were electrophoresed on 2.5% agarose gels to determine the genotypes of *IGF2* and *H19*. To determine the genotype of *H19*DMR, the 405-bp PCR products were purified using an agarose gel kit (Vitagene, China) and sequenced with the reverse primer by PCR on an ABI 377 sequence detection system at Shanghai Shenergy Biocolor Bioscience & Technology Co., Ltd., China.

Analysis of allelic-specific expression of IGF2 and H19

Heterozygous samples for *IGF2* and/or *H19* polymorphisms were analyzed for allelic expression by RT-PCR and RFLP. The RNAs were treated with RNase-free DNase (TaKaRa, Japan) before cDNA synthesis. No genomic DNA contamination was confirmed by performing the identical reaction simultaneously in the presence or absence of reverse transcriptase. Reverse transcription was performed in a volume of 25 μl using 2 μg of RNA, 2.5 μl of 10×RTase buffer (Promega), 200 U of M-MLV reverse transcriptase (Promega), 50 pM random hexamer (TaKaRa), and 20 U of RNasin (Promega), at 42 °C for 1 h. A 3-μl aliquot of the product was used as template to amplify the cDNAs with the same primers, reaction conditions, and temperature profiles of PCR as described for the above genotyping. The products of the RT-PCR were digested with ApaI, RsaI, or AluI and then electrophoresed as for genotyping.

Table 2
PCR primers used in this study

Primer	Sequence (5′ to 3′)	Annealing temperature (°C)	PCR product (bp)
Genotyping and allele expression of IGF2 polymorphism (ApaI)			
IGF2-758	CTTGGACTTTGAGTCAAATTGG	55	236
IGF2-993	CCTCCTTTGGTCTTACTGGG		
Genotyping and allele expression of H19 polymorphism (AluI)			
H19-10273	TCAGGAATCGGCTCTGGAAG	58	247
H19-10519	ATGATGTGGTGGCTGGTGGT		
Genotyping and allele expression of H19 polymorphism (RsaI)			
H19-12283	CCACCACATCATCCCAGAGC	58	397
H19-12679	GAATGCTTGAAGGCTGCTCC		
Genotyping of H19DMR polymorphisms (*Fig. 3*)			
H19-7925	GCACGGAATTGGTTGTAGTT	51	405
H19-8329	AGGCAATTGTCAGTTCAGTAA		
Cloning analysis of bisulfite-treated DNA (*Fig. 3*)			
H19-7769BT	GGAATAATGAGGTGTTTTAGTTTTA	51	602
H19-8370BT	CTAACCACTTAAAACTAAAAAAATC		
H19-7834BT	GTAGGGTTTTTGGTAGGTATAGAGT	51	504
H19-8337BT	CACTAAAAAAACAATTATCAATTC		

PCR primers are named for the gene they target and the position of the 5′ base as documented in GenBank (Accession No. X07868 for *IGF2* primers, AF125183 for all *H19* primers). Primers are labeled BT when they were designed to anneal to DNA that had been bisulfite treated. Optimal annealing temperatures were determined by PCR on a thermal cycler.

Bisulfite treatment of genomic DNA

Bisulfite modification was carried out based on the principle that bisulfite treatment of genomic DNA would efficiently convert unmethylated cytosines to uracil, while 5-methylcytosine remained unchanged [26]. To investigate the allele-specific methylation status of cytosines of *H19*DMR, the genomic DNAs of the samples that were heterozygous at *H19*DMR were required to be bisulfite treated and then amplified by PCR, finally cloned, and sequenced.

Two micrograms of genomic DNA was denatured in 50 μl of 0.2 M NaOH at 37 °C for 15 min, and then 30 μl of 10 mM hydroquinone and 520 μl of 3 M sodium bisulfite, both freshly prepared, were added. The solution was covered with liquid wax and incubated at 50 °C for 16 h. The bisulfite-treated DNAs were purified with a Wizard Cleanup kit (Promega), then denatured in 100 μl of 0.3 M NaOH at 37 °C for 5 min, and finally precipitated by ethanol. The purified DNA was dissolved in 50 μl distilled water, and 3 μl was used for each subsequent analysis.

Cloning and sequencing of bisulfite-treated DNA

We adopted the nested-PCR method to improve the specificity of amplification. Two primer pairs were designed for nested-PCR to amplify a region from 2263 to 1760 bp upstream of the *H19* transcription start site, which contains the sixth of seven CTCF-binding sites upstream of *H19* (Fig. 3A). The optimal annealing temperature for each primer pair is given in Table 2. Thermocycling was performed on the Mygene25 Plus thermal cycler (LongGene). An initial preheating step of 5 min at 95 °C was used to melt double-stranded DNA. A touchdown procedure followed, consisting of 45 s at 95 °C, annealing for 1 min at temperatures decreasing from 57 to 48 °C for the first 10 cycles (with 1 °C decrease for each cycle) and at 51 °C for the following 20 cycles, then 45 s at 72 °C, and ending with an extension step at 72 °C for 10 min. A total of 30 cycles were performed. A 3-μl sample of the first PCR products from 25 μl total volume was used as the template for the second PCR. The final 504-bp PCR products were separated on 1.5% agarose gel, purified using the V-gene gel extraction kit (Vitagene), subsequently cloned into a pMD18-T vector (TaKaRa) according to the manufacturer's instructions, and then transformed into JM109 *E. coli.* The DNA of plasmids from 10 to 20 random positive clones was sequenced for each individual.

Statistical analysis

Fisher's exact probabilities test was used to determine whether the epigenotypes (hyper-, medium-, and hypomethylated profiles) were associated with allelic expression of *IGF2* and *H19* (normal versus abnormal imprinting).

Acknowledgments

We thank Dr. J. Liu and J. Wang for assistance with the samples. This work was supported by a grant from the National Natural Science Foundation of China (No. 30470792).

References

[1] T.M. DeChiara, A. Efstratiadis, E.J. Robertson, A growth-deficiency phenotype in heterozygous mice carrying an insulin-like growth factor II gene disrupted by targeting, Nature 345 (1990) 78–80.
[2] T.M. DeChiara, E.J. Robertson, A. Efstratiadis, Parental imprinting of the mouse insulin-like growth factor II gene, Cell 64 (1991) 849–859.
[3] C.I. Brannan, E.C. Dees, R.S. Ingram, S.M. Tilghman, The product of the H19 gene may function as an RNA, Mol. Cell. Biol. 10 (1990) 28–36.
[4] Y. Zhang, B. Tycko, Monoallelic expression of the human H19 gene, Nat. Genet. 1 (1992) 40–44.
[5] Y. Jinno, et al., Mouse/human sequence divergence in a region with a paternal-specific methylation imprint at the human H19 locus, Hum. Mol. Genet. 5 (1996) 1155–1161.
[6] J.L. Thorvaldsen, K.L. Duran, M.S. Bartolomei, Deletion of the H19 differentially methylated domain results in loss of imprinted expression of H19 and Igf2, Genes Dev. 12 (1998) 3693–3702.
[7] C. Kanduri, et al., The 5′ flank of mouse H19 in an unusual chromatin conformation unidirectionally blocks enhancer–promoter communication. Curr. Biol. 10 (2000) 449–457.

[8] A.C. Bell, G. Felsenfeld, Methylation of a CTCF-dependent boundary controls imprinted expression of the Igf2 gene, Nature 405 (2000) 482–485.
[9] A.T. Hark, et al., CTCF mediates methylation-sensitive enhancer-blocking activity at the H19/Igf2 locus, Nature 405 (2000) 486–489.
[10] H. Sasaki, et al., Parental imprinting: potentially active chromatin of the repressed maternal allele of the mouse insulin-like growth factor II (Igf2) gene, Genes Dev. 6 (1992) 1843–1856.
[11] S. Rainier, et al., Relaxation of imprinted genes in human cancer, Nature 362 (1993) 747–749.
[12] H. Cui, et al., Loss of imprinting of insulin-like growth factor-II in Wilms' tumor commonly involves altered methylation but not mutations of CTCF or its binding site, Cancer Res. 61 (2001) 4947–4950.
[13] H. Nakagawa, et al., Loss of imprinting of the insulin-like growth factor II gene occurs by biallelic methylation in a core region of H19-associated CTCF-binding sites in colorectal cancer, Proc. Natl. Acad. Sci. U. S. A. 98 (2001) 591–596.
[14] H. Cui, et al., Loss of imprinting in colorectal cancer linked to hypomethylation of H19 and IGF2, Cancer Res. 62 (2002) 6442–6446.
[15] D. Takai, et al., Large scale mapping of methylcytosines in CTCF-binding sites in the human H19 promoter and aberrant hypomethylation in human bladder cancer, Hum. Mol. Genet. 10 (2001) 2619–2626.
[16] G.A. Ulaner, et al., Loss of imprinting of IGF2 and H19 in osteosarcoma is accompanied by reciprocal methylation changes of a CTCF-binding site, Hum. Mol. Genet. 12 (2003) 535–549.
[17] X. Li, et al., Expression levels of the insulin-like growth factor-II gene (IGF2) in the human liver: developmental relationships of the four promoters, J. Endocrinol. 149 (1996) 117–124.
[18] T.H. Vu, A.R. Hoffman, Promoter-specific imprinting of the human insulin-like growth factor-II gene, Nature 371 (1994) 714–717.
[19] S.S. Thorgeirsson, J.W. Grisham, Molecular pathogenesis of human hepatocellular carcinoma, Nat. Genet. 31 (2002) 339–346.
[20] T. Sohda, et al., In situ detection of insulin-like growth factor II (IGF2) and H19 gene expression in hepatocellular carcinoma, J. Hum. Genet. 43 (1998) 49–53.
[21] N. Iizuka, et al., Comparison of gene expression profiles between hepatitis B virus- and hepatitis C virus-infected hepatocellular carcinoma by oligonucleotide microarray data on the basis of a supervised learning method, Cancer Res. 62 (2002) 3939–3944.
[22] C.H. Lin, et al., Genome-wide hypomethylation in hepatocellular carcinogenesis, Cancer Res. 61 (2001) 4238–4243.
[23] Y. Saito, et al., Expression of mRNA for DNA methyltransferases and methyl-CpG-binding proteins and DNA methylation status on CpG islands and pericentromeric satellite regions during human hepatocarcinogenesis, Hepatology 33 (2001) 561–568.
[24] X. Li, et al., Disrupted IGF2 promoter control by silencing of promoter P1 in human hepatocellular carcinoma, Cancer Res. 57 (1997) 2048–2054.
[25] J. Sambrook, D.W. Russell, Molecular Cloning: a Laboratory Manual, 3rd ed., Cold Spring Harbor Laboratory Press, Cold Spring Harbor, NY, 2001.
[26] M. Frommer, et al., A genomic sequencing protocol that yields a positive display of 5-methylcytosine residues in individual DNA strands, Proc. Natl. Acad. Sci. U. S. A. 89 (1992) 1827–1831.
[27] C. Schwienbacher, et al., Gain of imprinting at chromosome 11p15: a pathogenetic mechanism identified in human hepatocarcinomas, Proc. Natl. Acad. Sci. U. S. A. 97 (2000) 5445–5449.
[28] M.J. O'Neill, The influence of non-coding RNAs on allele-specific gene expression in mammals, Hum. Mol. Genet. 14 (Spec. No. 2) (2005) R113–R120.
[29] R.A. Scelfo, et al., Loss of methylation at chromosome 11p15.5 is common in human adult tumors, Oncogene 21 (2002) 2564–2572.
[30] K. Poirier, et al., Loss of parental-specific methylation at the IGF2 locus in human hepatocellular carcinoma, J. Pathol. 201 (2003) 473–479.
[31] R. Kuzawa, et al., High frequency of inactivation of the imprinted H19 gene in "sporadic" hepatoblastoma, Int. J. Cancer 82 (1999) 490–497.
[32] Y. Yamasaki, et al., Neuron-specific relaxation of Igf2r imprinting is associated with neuron-specific histone modifications and lack of its antisense transcript Air, Hum. Mol. Genet. 14 (2005) 2511–2520.
[33] R.A. Drewell, et al., Deletion of a silencer element disrupts H19 imprinting independently of a DNA methylation epigenetic switch, Development 127 (2000) 3419–3428.
[34] R.A. Drewell, C.J. Goddard, J.O. Thomas, M.A. Surani, Methylation-dependent silencing at the H19 imprinting control region by MeCP2, Nucleic Acids Res. 30 (2002) 1139–1144.
[35] N. Engel, A.G. West, G. Felsenfeld, M.S. Bartolomei, Antagonism between DNA hypermethylation and enhancer-blocking activity at the H19 DMD is uncovered by CpG mutations, Nat. Genet. 36 (2004) 883–888.
[36] G.A. Ulaner, et al., CTCF binding at the insulin-like growth factor-II (IGF2)/H19 imprinting control region is insufficient to regulate IGF2/H19 expression in human tissues, Endocrinology 144 (2003) 4420–4426.
[37] I. Sandovici, et al., Familial aggregation of abnormal methylation of parental alleles at the IGF2/H19 and IGF2R differentially methylated regions, Hum. Mol. Genet. 12 (2003) 1569–1578.